Polymer Journal (2012) 44, 868–875

www.nature.com/pj

ORIGINAL ARTICLE

^{1}H MRI study of small-diameter silk vascular grafts in water

Shigeki Kuroki[1], Masahito Kanekiyo[2], Koji Yazawa[3], Kotaro Isobe[3] and Tetsuo Asakura[3]

Small-diameter vascular grafts (VG) made from silk fibroin (SF) fibers by a double-raschel knitting method were prepared by coating their interior and exterior with different materials, such as SF or polyurethane (PU). The ^{1}H spin density, ^{1}H spin–spin relaxation time (T_2) and diffusion coefficient (D) of the water molecules in the layer of the VG coated by these materials were non-destructively observed in water using ^{1}H NMR imaging. The inner and outer coating materials significantly affected the amount and mobility of water molecules in the VG. The water content of the SF-coated VG was considerably higher than that of PU-coated VG. The T_2 value of the water molecules in the SF-coated VG layer was smaller than that of the PU-coated VG, which means that the rotational motion of the water molecules in the layer of the SF-coated VG was restricted by the intermolecular interaction between the SF and water molecules. The diffusion coefficient (D) of the water molecules in the SF-coated VG layer was larger than that of the PU-coated VG, indicating that the water molecules were confined to the pores in the graft layer of the PU-coated VG.
Polymer Journal (2012) **44,** 868–875; doi:10.1038/pj.2012.77; published online 30 May 2012

Keywords: diffusion coefficient; ^{1}H MRI; silk fibroin; small-diameter vascular graft; T_2

INTRODUCTION

Vascular grafts (VG) prepared from expanded polytetrafluoroethylene or poly(ethylene terephthalate) (Dacron) have been used clinically for the revascularization of blood vessels with inner diameters $\geqslant$6 mm. However, the replacement of smaller vessels ($\leqslant$5 mm) with these synthetic materials leads to the failure of the grafts, mainly because of early thrombosis formation.[1,2] In addition, the synthetic materials that are commonly used lack growth potential, and long-term results have revealed several material-related failures; for example, stenosis, thromboembolization, calcium deposition and infection.[2] To overcome these limitations, various tissue-engineered VG have been developed, including poly-L-lactic acid, polyglycolic acid, polyurethane (PU), poly-e-caprolactone, cellulose, chitosan, poly(vinylalcohol) and their composites.[1,3–8] However, at present, no materials satisfy the strict requirements of small-diameter grafts.

Silk fibroin (SF) from *Bombyx mori* is one of the candidates for small-diameter artificial grafts because the high strength and toughness of SF fiber have led to a long history of use in sutures.[9] In our previous studies,[10–12] SF grafts proved to be effective, as VG implanted in rat models. Owing to the success of these *in vivo* experiments, it has become important to obtain information on the state and mobility of water molecules around and inside of the graft with respect to thrombosis.

NMR imaging (MRI)[13,14] is a useful technique for non-destructively obtaining μm-scale spatial information about probe molecules, such as water in bulk matter. For this reason, MRI has been successfully applied to polymer gel systems.[15–20] The contrast of the resulting images is produced by the difference in the ^{1}H spin density, ^{1}H spin–spin relaxation time (T_2) and diffusion coefficient (D). To develop an image, ^{1}H MRI non-destructively applies information about the number of water molecules in the VG from the ^{1}H spin density image and the mobility of water molecules in the VG from the ^{1}H T_2 and diffusion coefficient (D) images.

In this study, ^{1}H NMR imaging was used to observe the spatial distribution of the ^{1}H density, T_2 and the diffusion coefficient (D) of water molecules in small-diameter silk fibroin VG coated with different materials (SF and PU) in water, and differences in the amount and mobility of water in the layers of the grafts were identified.

EXPERIMENTAL PROCEDURE

Preparation of the VG from silk fibers

Raw silk fibers with silk sericin were used as the starting materials. The 4.0-mm diameter silk VG tube was prepared by a computer-controlled double-raschel knitting machine. The double-raschel-knitted silk tubes were degummed with a solution of sodium carbonate (0.1% *w/v*) and Marseille soap (0.2% *w/v*) at 95 °C for 120 min to remove silk sericin from the surface of the SF fiber. A Teflon rod was inserted into the SF graft tube so that the surface of the rod was covered with the SF fiber. The exteriors of the tubes were then coated with a SF aqueous solution or a PU solution. The outer-coated tubes were soaked in

[1]Department of Organic and Polymeric Materials, Tokyo Institute of Technology,Tokyo, Japan; [2]LSIC Co. Ltd. Idasugiyama-cho, Nakahara-ku, Kawasaki, Kanagawa, Japan and [3]Graduate School of Engineering, Tokyo University of Agriculture and Technology, Koganei, Tokyo, Japan
Correspondence: Dr S Kuroki, Department of Organic and Polymeric Materials, Tokyo Institute of Technology, 2-12-1 Ookayama, Meguro-ku, Tokyo 152-8552, Japan.
E-mail: skuroki@polymer.titech.ac.jp
Received 26 January 2012; revised 12 March 2012; accepted 14 March 2012; published online 30 May 2012

liquid N_2 and frozen at −80 °C for 1 h. Then, the tubes were vacuum dried overnight. This outer-coating process was repeated two times, after which the tubes were kept in an autoclave at 120 °C. After autoclaving, the tubes were soaked in water, the Teflon rod was withdrawn and the outer-coated silk tubes were dried at 50 °C. Next, the interiors of the tubes were soaked in SF, PU and SF + PU complex solutions, coating them in the same manner as the outer-coating. This outer and inner coating method is summarized in Figure 1.

We prepared several types of VG according to this coating method, as follows:

(1) VG-S/S: Both sides (interior and exterior of the graft) were coated with SF.
(2) VG-U/S: The exterior was coated with PU and the interior was coated with SF.
(3) VG-U/SU: The exterior was coated with PU and the interior was coated with SF and PU (1:1).
(4) VG-U/U: Both sides were coated with PU.

The final wall thickness of these grafts was 0.5 mm.

The cell-adhesive character was examined by cultivating human umbilical vein endothelial cells on plates coated with SF and PU, as shown in Figure 2. In this test, the surface of a 1.91-cm^2 well in a 24-well tissue culture plate was coated with SF and PU (0.47 mg per well). After drying overnight, 70% ethanol was applied to the dishes to insolubilize and sterilize the SF. Then, the ethanol was removed and the coated dishes were washed twice with phosphate-buffered saline. Before seeding the cells, the dishes were incubated at 37 °C in 5% CO_2. Then, 2×10^4 cells per well of human umbilical vein endothelial cells were added to each well. After a 3-h incubation in full growth medium (EBM-2) at 37 °C in a 5% CO_2 atmosphere, the unattached cells were removed by gently rinsing the wells twice. The cells were stained with calcein-AM stock solution (Dojindo Co., Kumamoto, Japan) and counted with a fluorescence microscope with the appropriate filters. High adhesive character was observed for the SF coating, but essentially no cell-adhesive character was observed for the PU coating (Figure 2).

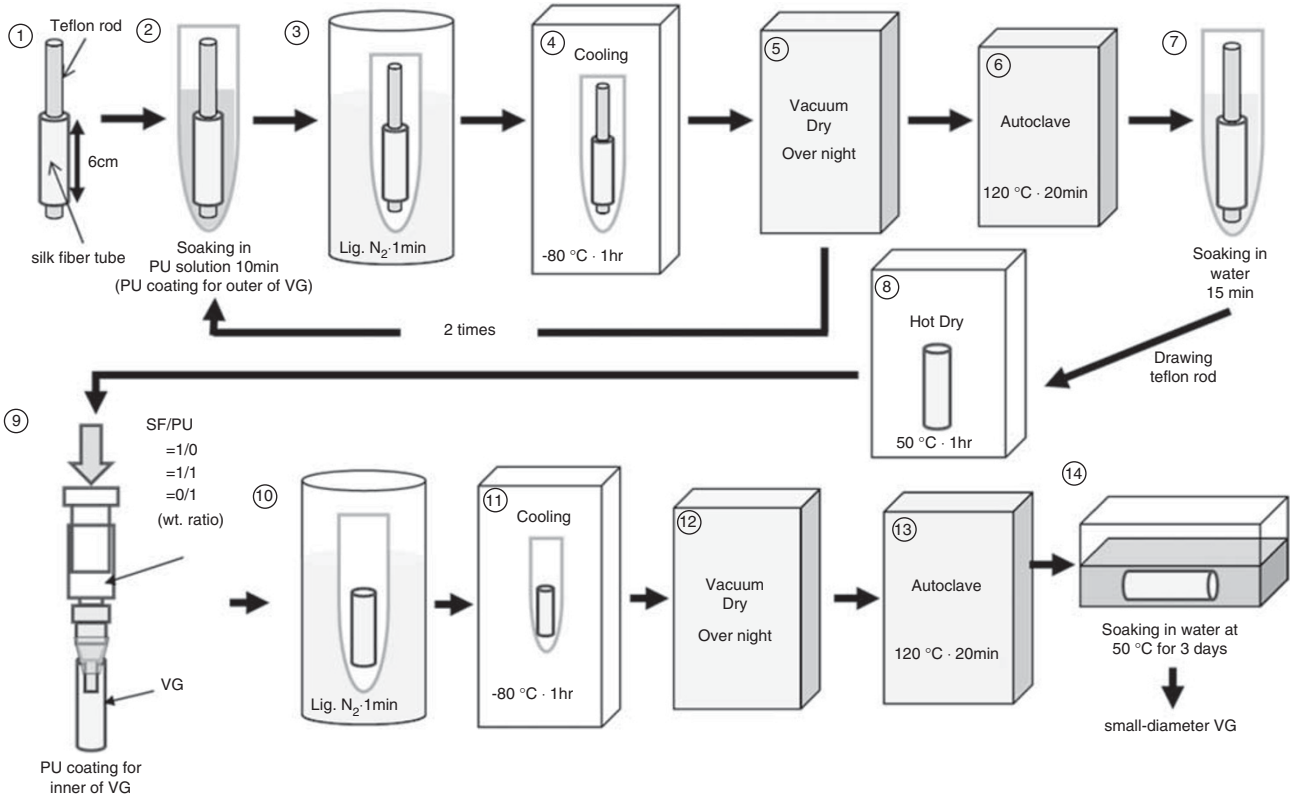

Figure 1 Typical coating method for VG.

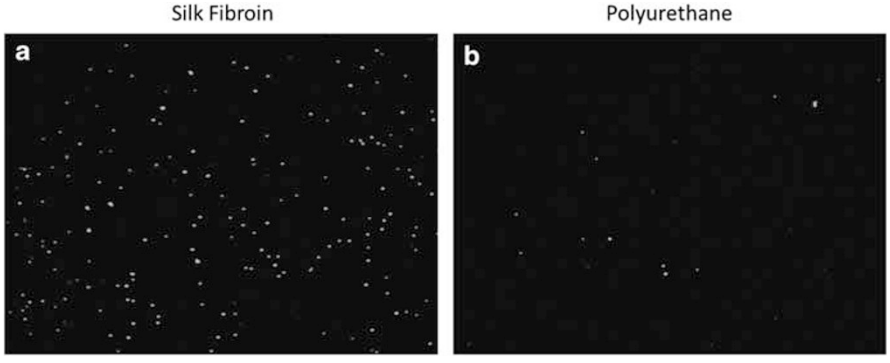

Figure 2 The cell-adhesive character of human umbilical vein endothelial cells on silk fibroin- or PU-coated plates.

MRI measurement

^{1}H NMR imaging measurements were carried out in a Bruker BioSpin Avance DSX 300 NMR spectrometer (Bruker BioSpin, Rheinstetten, Germany) with an imaging system operating at 300 MHz and 290 or 300 K. For the acquisition and processing of the NMR data, the ParaVision program supplied by Bruker Biospin was used. Two sample configurations were prepared. In the first, the VG were set in a 5-mm NMR tube (with an internal diameter of 4 mm), the exteriors of the VG were in direct contact with the glass tube and pure water was added to fill only the interior of the VG (inside-water) (Figure 3a). In the second configuration, the VG were set in an 8-mm NMR tube (with an internal diameter of 7 mm) and both the interiors and exteriors of the VG were filled with pure water (both-side water) (Figure 3b).

The ^{1}H spin density, ^{1}H spin–spin relaxation time (T_2) and diffusion coefficient (D) images were constructed with the NMR2CALC program supplied by LSIC Co. Ltd, Kawasaki, Japan.

RESULTS AND DISCUSSION

Spin-echo MR images of silk VG in inside-water case

Figure 4 shows spin-echo ^{1}H images of the silk VG, in which (a) shows VG-S/S and (b) shows VG-U/S. The echo time is 13.4 ms and the repetition time is 1 s. The data points constituted a 512×360 array for an image and the field of view (FOV) was 1.11 cm. The slice thickness was 0.5 mm. The ^{1}H signals in this experiment were mainly produced by the ^{1}H in the water, because the T_2 value of the SF is very short. The images in Figures 4a and b , which show the VG-S/S and VG-U/S samples that were inner-coated with SF, respectively, indicate that the brightness of the VG-S/S layer is greater than that of the VG-U/S layer. This result means that the VG-S/S layer contains a greater number of water molecules than the VG-U/S layer. This result shows that the outer-coating material also influences the amount of water in the VG.

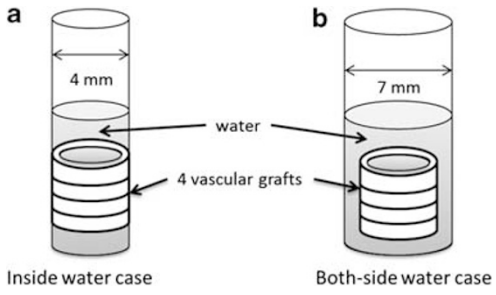

Figure 3 MR imaging sample tube of the VG in water used in this study.

The ^{1}H spin density and T_2 images of the silk VG the inside-water case constructed from several spin-echo ^{1}H NMR images

To perform a more quantitative analysis of the ^{1}H MRI data, we constructed the ^{1}H spin density (S_0) and T_2 images of the silk VG from the various echo times of the spin-echo ^{1}H NMR images. The echo times (τ) were 10.97, 21.94, 32.91, 43.88, 54.85, 65.82, 76.79, 87.76, 98.73 and 109.7 ms, and the repetition time was 1 s. The data points constituted a 256×256 array in an image and the FOV was 1.10 cm. The slice thickness was 0.5 mm. We used very long repetition time for T_1; consequently, we neglected the T_1 effect in the images. The signal intensity (S_τ) can be described by the following expression:

$$S_\tau = S_0 \exp(\tau/T_2) \quad (1)$$

From this equation, the ^{1}H spin density (S_0) and T_2 can be calculated from various echo time (τ) experiments.

Figure 5 shows the ^{1}H spin density (S_0) images of the silk VG, which are (a) VG-S/S, (b) VG-U/S, (c) VG-U/SU and (d) VG-U/U. The ^{1}H spin density in the VG-S/S layer is clearly greater than that of the VG-U/X layer (where X = S, SU and U). This result means that the amount of water in the VG-S/S layer is larger than that in the VG-U/X layer. From the SEM images, the outer coating material can be seen to permeate the silk graft layer.[12] As SF is a hydrophilic material and PU is a hydrophobic material, the amount of water in the VG-S/S layer is greater than that in the VG-U/X layer.

Figure 6 shows the T_2 images of the silk VG, (a) VG-S/S, (b) VG-U/S, (c) VG-U/SU and (d) VG-U/U. The ^{1}H T_2 of bulk water is approximately 45 ms in Figure 6. The T_2 images of VG-U/X (X = S, SU and U) show a T_2 data defect area (black area), which means that the area contained little or no water, and the initial intensity of the ^{1}H signal was very low. The data defect area increased as the content of PU in the coating increased. The T_2 of the VG-S/S was 30–37.5 ms, and that of VG-U/X (X = S, SU and U) was 35–45 ms. Thus, the rotational mobility of water in VG-U/X is slightly greater than that of VG-S/S because T_2 is associated with the rotational motion of water molecules. It is known that the intermolecular interaction between SF and water occurs through the formation of hydrogen bonds between the amide or carbonyl groups of SF molecules and water molecules,

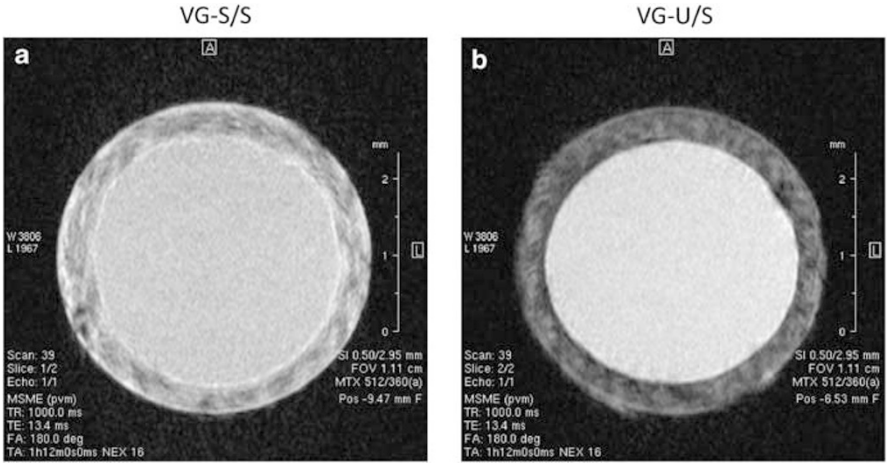

Figure 4 Spin-echo ^{1}H images of silk VG, which are (**a**) VG-S/S and (**b**) VG-U/S. The echo time was 13.4 ms and the repetition time was 1 s. The data points numbered 512×360 for an image and the FOV was 1.11 cm. The slice thickness was 0.5 mm.

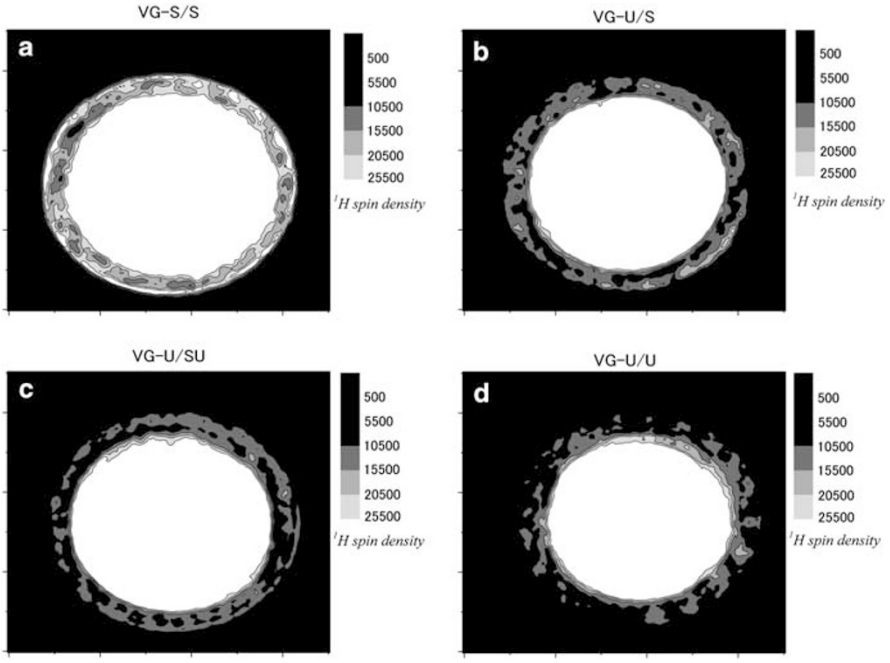

Figure 5 ^{1}H spin density images of silk VG, (**a**) VG-S/S, (**b**) VG-U/S, (**c**) VG-U/SU and (**d**) VG-U/U in the inside-water case.

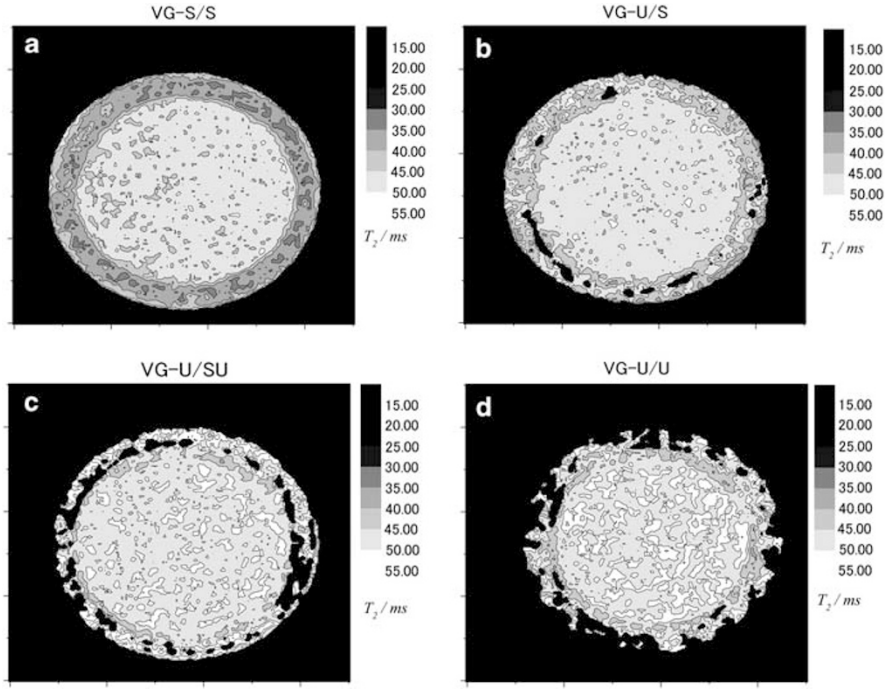

Figure 6 T_2 images of silk VG, (**a**) VG-S/S, (**b**) VG-U/S, (**c**) VG-U/SU and (**d**) VG-U/U in the inside-water case.

but that there is no intermolecular interaction between PU and water molecules. The rotational mobility of water molecules in a layer of VG-U/S is approximately the same as that of bulk water, but the rotational mobility of water molecules in a VG-S/S layer is restricted by the intermolecular interaction between the SF and water. These results show that the coating material affects both the amount and mobility of water in the layers of the VG.

The diffusion coefficient images of the silk VG in the inside-water case are constructed from several pulse-field gradient spin-echo ^{1}H NMR images

T_2 is associated with the rotational motion of water molecules, but the diffusion coefficient (D) is associated with the center of gravity translation of water molecules. These two parameters indicate the different types of dynamics available to water molecules.

Figure 7 shows the diffusion coefficient (D) images of silk VG, (a) VG-S/S, (b) VG-U/S, (c) VG-U/SU and (d) VG-U/U, that are constructed from several pulse-field gradient spin-echo ^{1}H NMR images with a field gradient pulse length of $\delta = 10$ ms, a gradient pulse separation of $\Delta = 25$ ms and field gradient strengths of $G = 0$, 20, 40, 60, 80 and 100 mT m^{-1}. The data points constitute a 128×128 array for an image and the FOV is 1.10 cm. The slice thickness is 0.5 mm.

The relationship between the echo signal intensity S_G and the pulse-field gradient parameters in the pulse-field gradient spin-echo method is given by the following expression:

$$S_G = S_0 \exp(-\gamma^2\delta^2G^2D(\Delta - \delta/3)) \quad (2)$$

where S_0 is the signal intensity in the absence of gradient pulses, γ is the ^{1}H magnetogyric ratio and D is the diffusion coefficient. The plots of $\ln(S_G/S_0)$ against $\gamma^2G^2\delta^2(\Delta - \delta/3)$ produce a straight line with a slope of $-D$. Therefore, the value D can be determined from this slope.

The value of D for bulk water is approximately 1.6×10^{-9} m^2 s^{-1} at 290 K in Figure 7. The value of D in the VG-S/S layer is 0.9–1.2 $\times$ 10^{-9} m^2 s^{-1} and it has a value of 0.4–0.5 $\times$ 10^{-9} m^2 s^{-1} in VG-U/X (X = S, SU and U). Thus, the value of D in the VG-U/X layer is smaller than that in the VG-S/S layer. These results are inconsistent with the T_2 results. However, as we mentioned before, T_2 is associated with the rotational motion of water molecules, and the diffusion coefficient (D) is associated with the center of gravity translation of water molecules. These two parameters describe the different types of dynamics of water molecules. The T_2 experiment shows that there is no intermolecular interaction between the PU and the water molecules. The smaller D value of the water in VG than that of bulk water shows that the water in the VG diffuses through pores. The D image shows that the water molecules are confined to pores, and the restricted diffusion[21] of the water molecules occurs in the graft layer. The size of the pores in the VG-U/X is smaller than the pore size in VG-S/S.

^{1}H spin density and T_2 images of silk VG in both-side water case constructed from several spin-echo ^{1}H NMR images

In the previous experiment, we filled only the inside of the VG with pure water. However, in the *in vivo* case, the outside of the grafts was also wet. We prepared both the interior and exterior of the grafts by filling with pure water (both-side water; Figure 3b). The ^{1}H spin density (S_0) and T_2 images of the silk VG were constructed from the various echo time spin-echo ^{1}H NMR images. The echo times (τ) were 10, 20, 30, 40, 50, 60, 70, 80, 90, 100, 110, 120, 130, 140, 150 and 160 ms, and the repetition time was 1 s. The data points constituted a 256×256 array for an image and the FOV was 1.10 cm. The slice thickness was 0.5 mm.

Figure 8 shows the ^{1}H spin density (S_0) images of the silk VG, (a) VG-S/S, (b) VG-U/S, (c) VG-U/SU and (d) VG-U/U. The ^{1}H spin density in the VG-S/S layer is clearly higher than that of the VG-U/X (X = S, SU, U) layer, and the amount of water in the VG-S/S layer is greater than that of the VG-U/X. This result is the same as that of the inside-water case. As SF is a hydrophilic material and PU is a hydrophobic material, the amount of water in the VG-S/S layer is larger than that of the VG-U/X layer.

Figure 9 shows T_2 images of the silk VG, (a) VG-S/S, (b) VG-U/S, (c) VG-U/SU and (d) VG-U/U. The ^{1}H T_2 of bulk water in this experiment is approximately 45 ms. The T_2 of the VG-S/S layer is 30–37.5 ms, and that of VG-UX (X = S, SU and U) is 35–45 ms. The larger T_2 area increases in size as the PU content of the coating increases. This trend means that the mobility of water in VG-U/X is higher than its mobility in VG-S/S. This result is the same as that of the inside-water case. It is known that intermolecular interactions exist between SF and water (an effect of the hydrogen bond between the amide or carbonyl groups of SF molecules and water molecules), but there is no intermolecular interaction between PU and water. The rotational mobility of water molecules in the VG-U/S layer is nearly equal to that of bulk water, but the mobility of the water molecules in the VG-S/S layer is restricted by the intermolecular interaction between the SF and water. These results show that the coating material affects the amount and mobility of water in the VG layers.

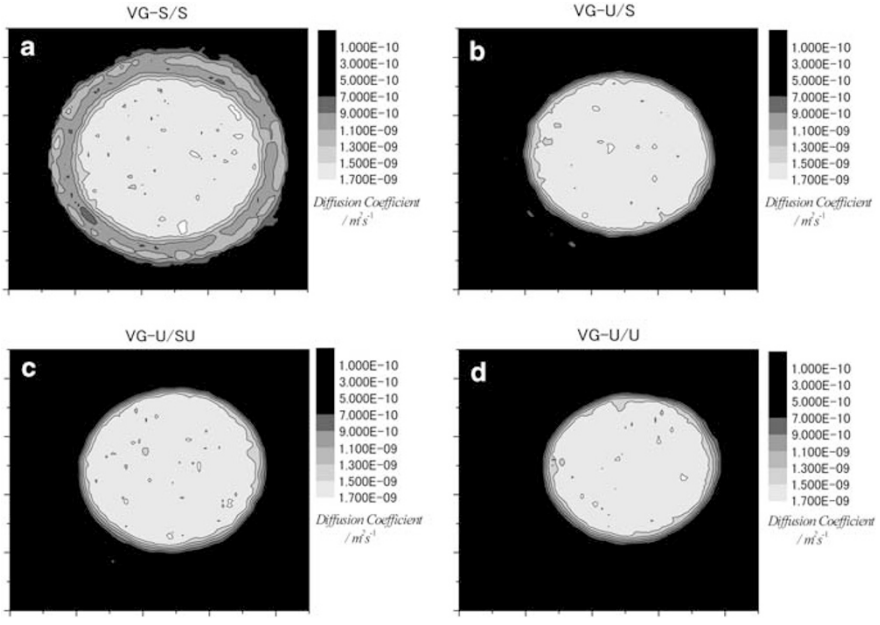

Figure 7 Diffusion coefficient (D) images of silk VG, (**a**) VG-S/S, (**b**) VG-U/S, (**c**) VG-U/SU and (**d**) VG-U/U in the inside-water case.

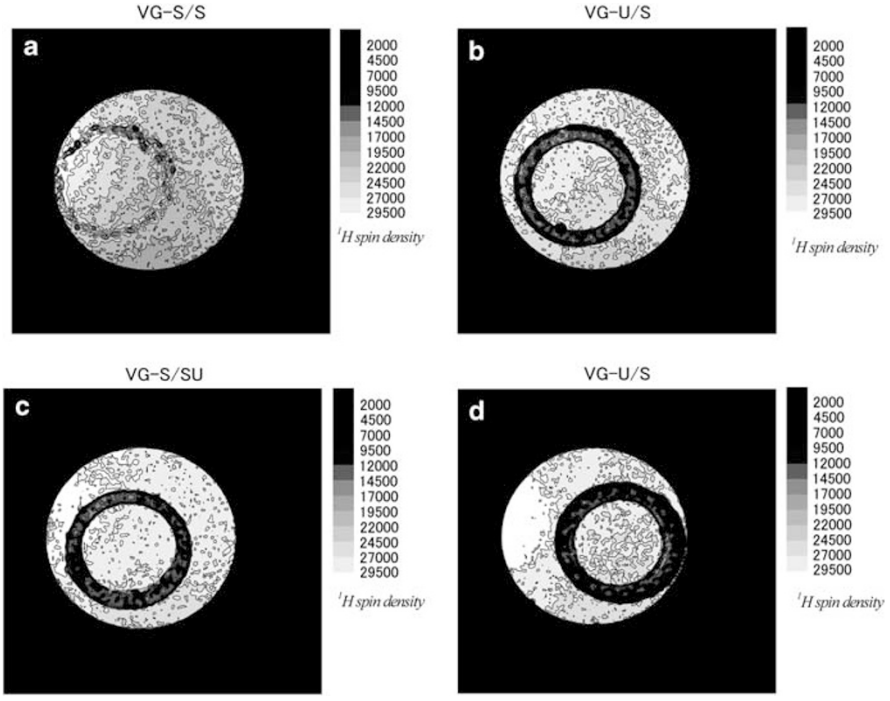

Figure 8 ^{1}H spin density images of silk VG, (**a**) VG-S/S, (**b**) VG-U/S, (**c**) VG-U/SU and (**d**) VG-U/U in the both-side water case.

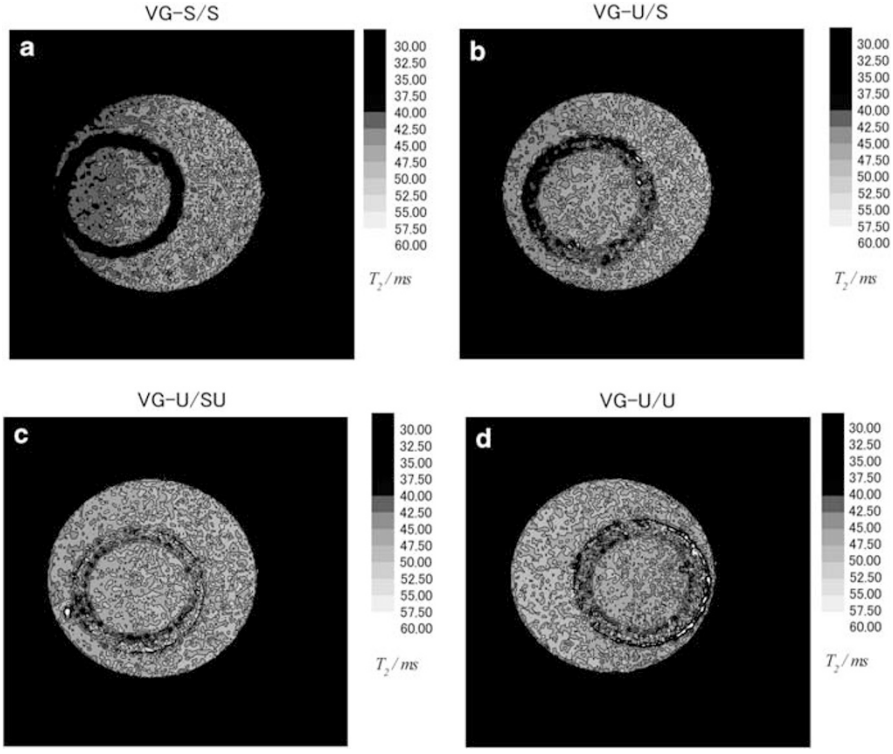

Figure 9 T_2 images of silk VG, (**a**) VG-S/S, (**b**) VG-U/S, (**c**) VG-U/SU and (**d**) VG-U/U in the both-side water case.

The diffusion coefficient images of the silk VG in the both-side water case were constructed from several pulse-field gradient spin-echo ^{1}H NMR images

Figure 10 shows the diffusion coefficient (D) images of silk VG, (a) VG-S/S, (b) VG-U/S, (c) VG-U/SU and (d) VG-U/U, that were constructed from several pulse-field gradient spin-echo ^{1}H NMR images with a field gradient pulse length of $\delta = 5$ ms, a gradient pulse separation of $\Delta = 10$ ms, and field gradient strengths of $G = 0$, 30, 60, 90, 120, 150, 180, 210, 240 and 270 mT m^{-1}. The data points constituted a 128×128 array

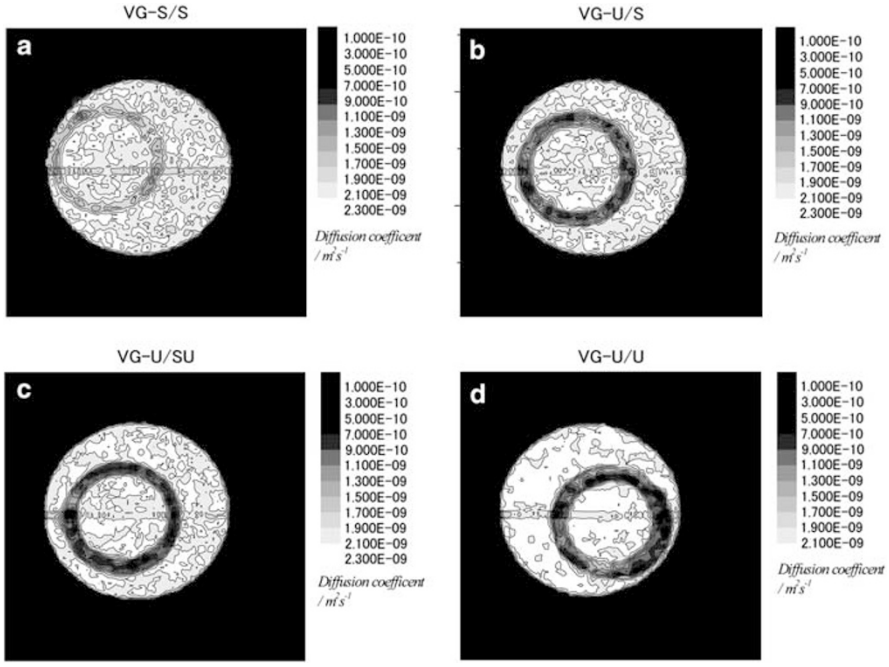

Figure 10 Diffusion coefficient (*D*) images of silk VG, (**a**) VG-S/S, (**b**) VG-U/S, (**c**) VG-U/SU and (**d**) VG-U/U in the both-side water case.

for an image and the FOV was 1.10 cm. The slice thickness was 0.5 mm.

The *D* value of bulk water is approximately $2.0 \times 10^{-9}\,m^2\,s^{-1}$ at 300 K in Figure 10. The *D* value in the VG-S/S layer is $1.5–1.9 \times 10^{-9}\,m^2\,s^{-1}$, and the value in VG-U/X (X = S, SU and U) is $0.7–1.3 \times 10^{-9}\,m^2\,s^{-1}$. The *D* value in the VG-U/X layer is significantly smaller than that in the VG-S/S layer. The *D* imaging results show that the water molecules are confined in a closed porous medium, and restricted diffusion occurs in the graft layers. The pore size in VG-U/X is smaller than that in VG-S/S.

CONCLUSIONS

The spatial distribution of the ^{1}H spin density T_2 and the diffusion coefficient (*D*) of water molecules in the layers of small-diameter silk fibroin VG coated with different materials (SF and PU) in water were successfully identified by ^{1}H NMR imaging. The water content of the SF-coated VG was higher than that of the PU-coated VG. The T_2 of the water molecules in the SF-coated VG layer was smaller than that of the PU-coated VG, which means the rotational motion of the water in the SF-coated VG layer was restricted by the intermolecular interaction between the SF and the water molecules. The diffusion coefficient (*D*) of the water molecules in the PU-coated VG layer was smaller than that of the SF-coated VG, and the water molecules were confined to the pores in the graft layer.

ACKNOWLEDGEMENTS

We acknowledge financial support from a Grant-in-Aid for Scientific Research from the Ministry of Education, Science, Culture and Sports of Japan (23245045) and (21550112), and the Agri-Health Translational Research Project from the Ministry of Agriculture, Forestry and Fisheries.

1 Yokota, T., Torikai, H., Matsumiya, G., Kuratani, T., Sakaguchi, T., Iwai, S., Shirakawa, Y., Torikai, K., Saito, A., Uchimura, E., Kawaguchi, N., Matsuura, N. & Sawa, Y. In situ tissue regeneration using a novel tissue-engineered, small-caliber vascular graft without cell seeding. *J. Thorac. Cardiovasc. Surg.* **136,** 900–907 (2008).
2 Venkatraman, S., Boey, F. & Lao, L. L. Implanted cardiovascular polymers: natural, synthetic and bio-inspired. *Prog. Polym. Sci.* **33,** 853–874 (2008).
3 Francois, S., Chakfe, N., Durand, B. & LAroche, G. A poly(L-lactic acid) nanofibre mesh scaffold for endothelial cells on vascular prostheses. *Acta Biomater.* **5,** 2418–2428 (2009).
4 Schumann, D. A., Wippermann, J., Klemm, D. O., Kramer, F., Koth, D., Kosmehl, H., Wahlers, T. & Selehi-Gelani, S. Artificial vascular implants from bacterial cellulose: preliminary results of small arterial substitutes. *Cellulose* **16,** 877–885 (2009).
5 Qiu, Y. Z., Zhang, N., Kang, Q., An, Y. H. & Wen, X. J. Fabrication of permeable tubular constructs from chemically modified chitosan with enchanced antithrombogenic property. *J. Biomed. Mater. Res. B Appl. Biomater.* **90B,** 668–678 (2009).
6 Liu, Y., Vrana, N. E., Cahill, P. A. & McGuinness, G. B. Physically crosslinked composite hydrogels of PVA with natural macromolecules: structure, mechanical properties, and endothelial cell compatibility. *J. Biomed. Mater. Res. B Appl. Biomater.* **90B,** 492–502 (2009).
7 Mirenski, T. L., Nelson, G. N., Brennan, M. P., Roh, J. D., Hibino, N., Yi, T., Shinoka, T. & Breuer, C. K. Tissue-engineered arterial grafts: long-term results after implantation in a small animal model. *J. Pediatr. Surg.*. **44,** 1127–1133 (2009).
8 Grasl, C., Bergmeister, H., Stoiber, M., Schima, H. & Weigel, G. Electrospun polyurethane vascular grafts: *in vitro* mechanical behavior and endothelial adhesion molecule expression. *J. Biomed. Mater. Res.* **A93A,** 716–723 (2010).
9 Altman, G. H., Diaz, F., Jakuba, C., Carabro, T., Horan, R. L., Chen, J., Lu, H., Richmond, J. & Kaplan, D. L. Silk-based biomaterials. *Biomaterials* **24,** 401–416 (2003).
10 Enomoto, S., Sumi, M., Kajimoto, K., NAkazawa, Y., Takahashi, R., Takahashi, C., Asakura, T. & Sata, M. Long-term patency of small-diameter vascular graft made form fibroin, a silk-based biodegradable material. *J. Vasc. Surg.* **51,** 155–164 (2010).
11 Sato, M., Nakazawa, Y., Takahashi, R., Tanaka, K., Sata, M., Aytemiz, D. & Asakura, T. Small-diameter vascular grafts on Bombyx mori silk fibroin prepared by a combination of electrospinning and sponge coating. *Mater. Lett.* **64,** 1786–1788 (2010).
12 Yagi, T., Sato, M., Nakazawa, Y., Tanaka, K., Sata, M., Itoh, K., Takagi, Y. & Asakura, T. Preparation of double-raschel knitted silk vascular grafts and evaluation of short-term function in a rat abdominal aorta. *J. Artif Organs.* **14,** 89–99 (2011).
13 Callaghan, P. T. *Principles of Nuclear Magnetic Resonance Microscopy* (Oxford University Press, Oxford, 1991).
14 Blümich, B *NMR Imaging of Materials.* (Clarendon Press, New York, 2000).

15 Yasunaga, H., Kurosu, H. & Ando, I. Spatial information on a polymer gel as studied by proton NMR imaging. 1. Image analysis of stress-strain. *Macromolecules.* **25,** 6505–6509 (1992).
16 Shibuya, T., Yasunaga, H., Kurosu, H. & Ando, I. Spatial information on a polymer gel as studied by ^{1}H NMR imaging. 2. Shrinkage by the application of an electric field to a polymer gel. *Macromolecules* **28,** 4377–4382 (1996).
17 Yamazaki, A., Hotta, Y., Kurosu, H. & Ando., I. Image analysis of the spatial distribution of paramagnetic Mn2+/ions in a PMAA gel with the application of an electric field by an ^{1}H NMR imaging method. *Polymer* **39,** 1511–1514 (1998).
18 Kanekiyo, M., Kobayashi, M., Ando, I., Kurosu, H. & Amiya, S. A study of solvent exchange process in (ethylene-vinyl alcohol) copolymer gels by a proton nuclear magnetic resonance spectroscopy imaging method. *J. Applied Polym. Sci.* **86,** 504–508 (2002).
19 Yokota, S., Sasaki, A., Hotta, Y., Yamane, Y., Kimura, H., Kuroki, S. & Ando, I. Image analysis of the spatial distribution of paramagnetic Pr3+ ions in a polymer gel by a ^{1}H-chemical shift NMR imaging method. *Macromol. Symp.* **207,** 105–109 (2004).
20 Yamane, Y., Koizumi, S., Kuroki, S. & Ando, I. Structural characterization of channel cavities with micrometer-scale diameters in highly-oriented polypeptide gels by three-dimensional NMR imaging and diffusion NMR methods. *J. Mol. Struct.* **739,** 137–143 (2005).
21 Price, W. S. Gradient NMR. *Ann. Rep. NMR Spectrosc.* **32,** 53–142 (1996).